Reprinted from:

CONTRIBUTION
SERIES

91-008

ELSEVIER SCIENCE PUBLISHERS B.V.
AMSTERDAM

Chemical Geology, 92 (1991) 1–20
Elsevier Science Publishers B.V., Amsterdam

Use of nonparametric ranking statistics to characterize magmatic and post-magmatic processes in the eastern South Mountain Batholith, Nova Scotia, Canada

M.A. MacDonald [a] and D.B. Clarke [b]

[a] *Nova Scotia Department of Mines and Energy, P.O. Box 1087, Halifax, N.S. B3J 2X1, Canada*
[b] *Department of Geology, Dalhousie University, Halifax, N.S. B3H 3J5, Canada*

(Received November 8, 1989; revised and accepted July 16, 1990)

ABSTRACT

MacDonald, M.A. and Clarke, D.B., 1991. Use of nonparametric ranking statistics to characterize magmatic and post-magmatic processes in the eastern South Mountain Batholith, Nova Scotia, Canada. In: A. Peccerillo (Guest-Editor), Geochemistry of Granitoid Rocks. Chem. Geol., 92: 1–20.

The South Mountain Batholith is a large, post-tectonic, peraluminous, granitoid complex consisting of many coalesced plutons. Compositions range from biotite granodiorite, through two-mica monzogranite, to muscovite leucogranite. Application of the non-parametric Spearman rank correlation coefficient (SRCC) statistic to major- and trace-element chemical data from one large pluton (the Halifax Pluton), and to two different groups of much smaller leucogranitoid bodies, shows strongly different correlation coefficients in the three groups. The Halifax Pluton shows strong SRCCs between compatible elements (Ba, Sr, Zr, Sc, V, La) and weak SRCCs for the incompatible elements (Rb, Ta, Nb, Li, F, Sn). The leucogranites generally show correlations opposite to the Halifax Pluton, and also show some strong correlations between elements that were poorly correlated in it (Na, K, Li, P). Non-geological controls (such as closure, dissimilar compositional ranges, dissimilar groupings, and differing analytical precisions) cannot account for the observed differences between the magnitudes and signs of the correlation coefficients in the three groups. On the other hand, geological controls (principally magmatic vs. hydrothermal) do explain most of the differences in the correlation coefficients, and the transition between magmatic and hydrothermal control is apparent. Spearman rank correlation coefficients can be used with compositional data drawn from populations with non-normal distributions: to provide a comprehensive and rapid, non-graphical assessment of inter-element correlations; to quantify these inter-element relationships; and to both identify processes, and to gauge their relative contributions to the observed compositions.

1. Introduction

The South Mountain Batholith (SMB) is a large (approx. 10,000 km^2), post-tectonic, Upper Devonian, peraluminous granitoid complex that cuts mainly flyschoid metasedimentary rocks of the Cambro–Ordovician Meguma Group. Many studies have shown that fractional crystallization controls chemical variation in most of the SMB (see Clarke and Muecke, 1985 for a review), and also that variable degrees of post-magmatic hydrothermal alteration (e.g. greisenization, albitization, etc.) modified the compositions produced by magmatic processes (Clarke and Chatterjee, 1988). Recent detailed mapping, followed by extensive petrographic and analytical work, provides a large geochemical database (MacDonald and Horne, 1988; Ham et al., 1989). This paper applies non-parametric Spearman rank correlation coefficients (SRCC) to a selected group of the new chemical analyses in order to quantify the degree of inter-element correlation in a single pluton (the Halifax Pluton, HP) showing a range of compositions from granodiorite to monzogranite,

0009-2541/91/$03.50 © 1991 Elsevier Science Publishers B.V. All rights reserved.

92-02620/

to quantify the degree of inter-element correlation in two suites of compositionally restricted leucogranites, and to assess the reasons for these correlations in terms of magmatic and post-magmatic processes. We also examine the influences of other factors on the inter-element correlations.

2. Methods

2.1. Analytical techniques

Analytical techniques include a combination of methods and laboratories. Major elements and Ba, Rb, Sr, Y, Zr, Nb, Pb, Zn, Cu, V, Ga, and Sn were done by XRF at the Nova Scotia Regional XRF Centre, Halifax. Other trace elements (Hf, Ta, Sc, La, Th, U, As, W) were done by INAA, Li by AA, F by specific ion electrode, and B by DC plasma emission by Bondar Clegg in Ottawa (Ham et al., 1989). Lower limits of detection for trace elements are 5 ppm or less for XRF, except Pb (10 ppm), and 1 ppm or less for the other techniques, except F (20 ppm) and B (10 ppm).

2.2. Non-parametric statistical techniques

A geochemical analysis transforms a rock into a vector of numbers. To realize the full taxonomic, petrogenetic, and economic potential of this elegant transformation, petrologists use the compositional data in a variety of ways, ranging from the traditional techniques of graphical interpretation and elementary statistics (e.g. mean, standard deviation, and range), to high-level bivariate and multivariate techniques.

Conventional parametric statistical techniques (e.g. *t*-test, *F*-test, Pearson correlation coefficient) require that observations be drawn from normally distributed populations with similar variance (Siegel, 1956). For example, some other parametric techniques (discriminant function analysis, factor analysis) have been used to evaluate subdivisions of the SMB (Smith, 1979; Chatterjee et al., 1983; Horne et al., 1989), and to effect regional correlations (Richard and Clarke, 1989).

In contrast, nonparametric techniques are not limited by the form of the distribution and, therefore, are more appropriate for geological data sets that typically display lognormal or exponential distributions, or that may contain more than one population (e.g. unaltered and altered samples). Henley (1981, p. 2) concluded that nonparametric statistical techniques are "robust with respect to departures from the ideal case, such as skewed populations and spatial trends". Similarly, Gibbons (1971) indicated that "with so-called 'dirty data' (i.e. analytically imprecise), most nonparametric techniques are, relatively speaking, much more appropriate than parametric methods". Several workers have used nonparametric techniques to evaluate geochemical trends and anomalies in stream sediments (Rogers and MacDonald, 1984; O'Connor et al., 1988), lake sediments and glacial tills (Rogers et al., 1984), and glacial tills and bedrock (Graves et al., 1988). Henley (1981) applied nonparametric statistics to the calculation of ore reserves. However, there are very few examples of the use of nonparametric statistics in igneous petrology.

In this paper we employ the nonparametric Spearman rank correlation coefficient (SRCC) using SYSTAT (Wilkinson, 1988). To calculate SRCC for a group of N samples containing several variables (e.g. X, Y, Z), each variable is first ranked from the highest to the lowest values using sequential integers, thus eliminating any effects of data distribution. A measure of the correlation between two variables (e.g. X and Y) is calculated by comparing the rank of one variable (e.g. $Y_i = Y_1, Y_2 \ldots, Y_N$) with the rank of another variable (e.g. $X_i = X_1, X_2 \ldots, X_N$), where X's and Y's are merely permutations of the first N integers (Yule and Kendall, 1965). The differences between the ranks $D_i = X_i - Y_i$ for $i = 1 - N$ is then used to calcu-

late the SRCC using the following equation (Henley, 1981):

$$r_s = 1 - \frac{6 \times \Sigma D_i^2}{N^3 - N}$$

Perfect positive correlation ($r_s = +1$) occurs when $X_1 = Y_1, X_2 = Y_2, \ldots, X_N = Y_N$. Perfect negative correlation ($r_s = -1$) occurs when $X_1 = Y_N, X_2 = Y_{N-1}, \ldots, X_N = Y_1$.

In contrast to SRCC, the parametric Pearson product-moment correlation coefficient uses actual values of each variable instead of sequential integers. The values for each ranked pair are then compared to the respective means of each population. Pearson calculations are therefore very sensitive to skewed, non-Gaussian data sets that may contain highly anomalous or outlier values.

Compositional variations in most granitoid complexes result from a combination of physical and chemical processes including fractional crystallization, assimilation, wall-rock

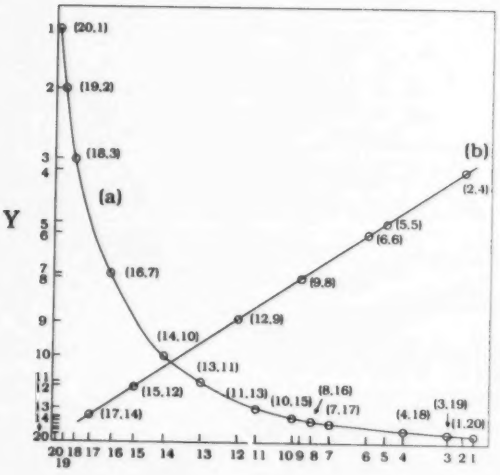

Fig. 1. Theoretical plot of an exponential curve (a) and a linear array (b). Regardless of the sample distribution, the SRCC will always equal -1 for (a) and $+1$ for (b). A composite data set with 13 samples from (a) and 7 samples from (b) has been created. Each sample has been ranked for both X and Y variables (e.g. X_1, X_2, ..., X_{20}) with respective ranks plotted in parentheses. The SRCC for the composite data set ($N = 20$) is -0.511.

TABLE 1

Spearman rank correlation coefficient (SRCC) significance levels corresponding to data sets of varying sample number (after Rogers et al., 1984). |SRCCs| > 0.56 are significant at the 99th confidence interval for a data set containing 18 samples (e.g. AL). Only |SRCCs| > 0.60 are considered significant in this paper

N	Significance level (one-tailed test)	
	0.05	0.01
4	1.00	1.00
5	0.90	0.94
6	0.83	0.89
7	0.71	0.83
8	0.64	0.78
9	0.60	0.75
10	0.56	0.71
12	0.51	0.65
14	0.46	0.60
16	0.43	0.56
18	0.40	0.53
20	0.38	0.51
22	0.36	0.49
24	0.34	0.47
26	0.33	0.45
28	0.32	0.43
30	0.31	0.43

interaction, flow segregation, crystal settling, magma mixing, and hydrothermal alteration. Each of these processes will have a characteristic effect on the final composition of a pluton and may generate unique inter-element correlations that can be detected using SRCCs. If fractional crystallization occurred within a granitoid pluton, in isolation from other processes, all inter-element SRCCs should be $+1$ or -1 (e.g. curve (a) in Fig. 1 which has $r_s = -1$), unless changes in the mineral phases crystallizing from the melt cause reversals in the enrichment or depletion trends, or in the case where several samples have the same composition for one or more variables (tied observations of Siegel, 1956). Similarly, intense single-process hydrothermal alteration could obliterate the pre-existing SRCCs produced by magmatic processes (e.g. fractional crystallization) and could produce its own characteristic set of SRCCs of $+1$ and -1 (e.g.

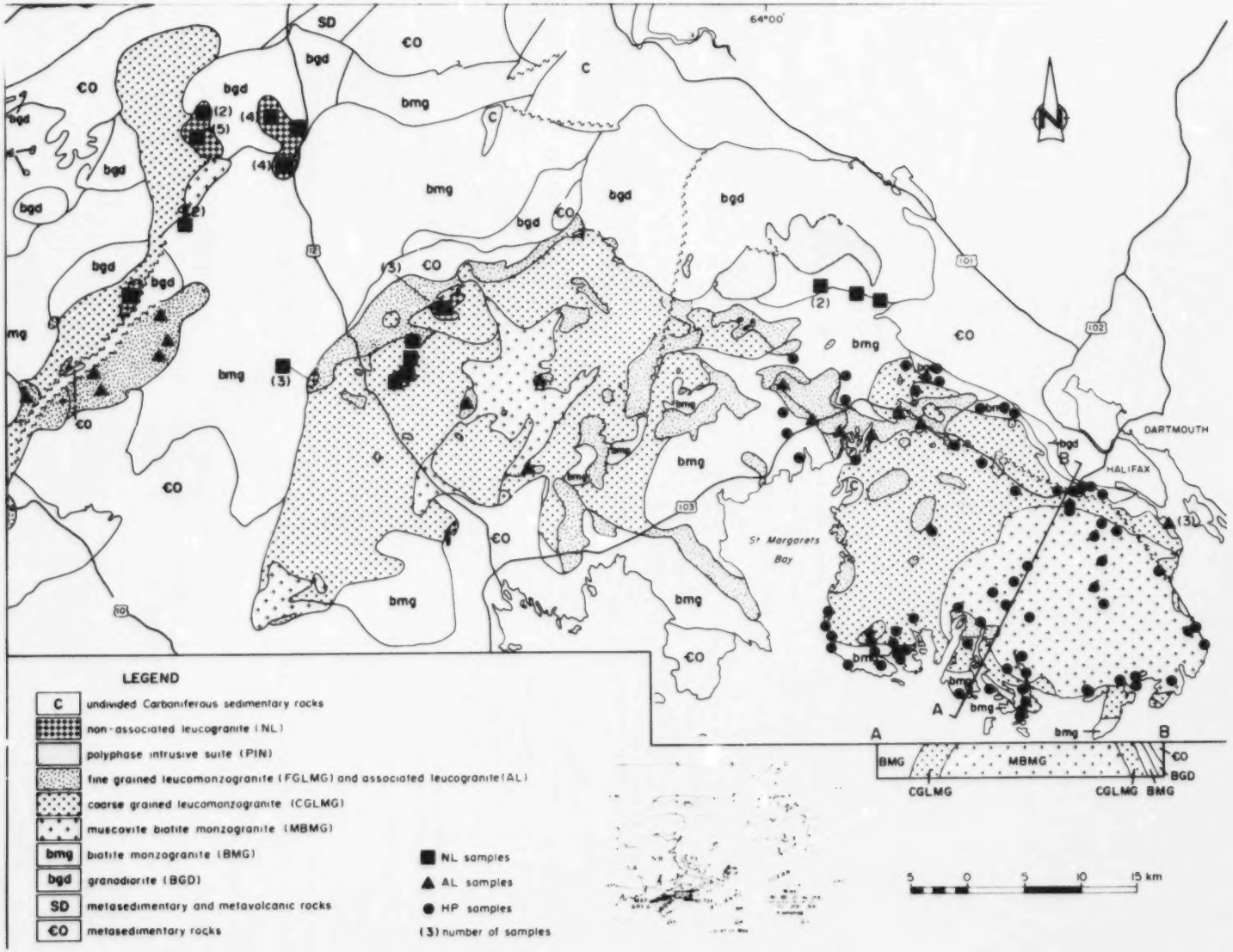
64°00'
SD
bgd
bmg
C
CO
(2)
(4)
(5)
(3)
DARTMOUTH
HALIFAX
St Margarets Bay
A
B
BMG
MBMG
CGLMG
BGD
5 0 5 10 15 km
LEGEND
C undivided Carboniferous sedimentary rocks
non-associated leucogranite (NL)
polyphase intrusive suite (PIN)
fine grained leucomonzogranite (FGLMG) and associated leucogranite (AL)
coarse grained leucomonzogranite (CGLMG)
muscovite biotite monzogranite (MBMG)
bmg biotite monzogranite (BMG)
bgd granodiorite (BGD)
SD metasedimentary and metavolcanic rocks
CO metasedimentary rocks
NL samples
AL samples
HP samples
(3) number of samples

curve (b) in Fig. 1 which has $r_s = +1$). However, the elemental pairs, signs, and slopes on bivariate plots for these correlations would undoubtedly differ from those produced by magmatic processes. The combination of two or more processes in a granitic pluton should generate $|SRCCs| < 1$, e.g. all the data in Fig. 1 have $r_s = -0.51$.

The data sets employed in this paper consist of relatively small populations with as few as 18 samples. Siegel (1956) concluded that there is no alternative to nonparametric techniques when sample size is small, unless the exact distribution of the data is known. A measure of the significance of SRCCs for various sized data sets (Table 1) has been adopted from Rogers et al. (1984). For data sets with more than 18 samples a SRCC greater than 0.56 is significant at the 99th confidence interval. For the purposes of this paper we have only considered absolute values of SRCC greater than 0.60.

3. General geology of the SMB

Previous studies of the SMB (Clarke and Muecke, 1985; Clarke and Chatterjee, 1988; Smith et al., 1986 and references therein) were based upon reconnaissance mapping or detailed mapping over restricted areas. Recent detailed geological mapping has delineated approximately 100 discrete bodies in the eastern SMB ranging from <1 to 1000 km^2. Subdivision of rocks was based upon proportions of quartz–alkali feldspar–plagioclase (QAP) according to the scheme of Streckeisen (1976), variations in texture, grain size, and the modal abundances of biotite, muscovite and feldspar megacrysts. These bodies were then grouped into seven main rock types including, in order of decreasing ferromagnesian mineral content

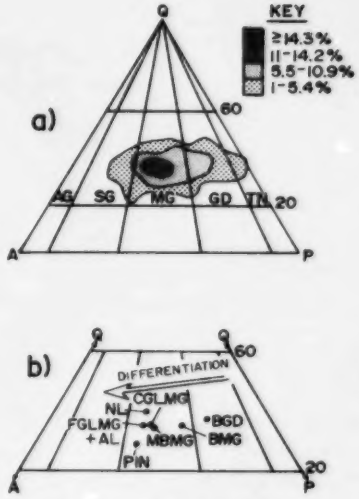

Fig. 3. a. Contoured density plot of 452 modal quartz–alkali feldspar–plagioclase (QAP) determinations from the entire SMB (after MacDonald et al., 1989). The SMB is predominantly composed of monzogranite (*MZ*) with lesser granodiorite (*GD*) and subordinate syenogranite (*SG*) and tonalite (*TN*; fields after Streckeisen, 1976). b. Average QAP compositions for biotite granodiorite (*BGD*), biotite monzogranite (*BMG*), muscovite–biotite monzogranite (*MBMG*), coarse-grained leucomonzogranite (*CGLMG*, polyphase intrusive suite (*PIN*), fine-grained leucomonzogranite (*FGLMG*), associated leucogranite (*AL*), and non-associated leucogranite (*NL*) from the entire SMB (after MacDonald et al., 1989). The data define a trend from least differentiated BGD with the lowest A/P to most differentiated FGLMG, AL, PIN, and NL with the highest A/P.

(biotite, cordierite, garnet): biotite granodiorite (BGD); biotite monzogranite (BMG); muscovite–biotite monzogranite (MBMG); coarse-grained leucomonzogranite (CGLMG); polyphase intrusive suite (PIN); fine-grained leucomonzogranite (FGLMG); and leucogranite (LUGR). Leucomonzogranitic rocks contain 2–6% ferromagnesian minerals (mostly biotite), whereas leucogranite contains less than 2% ferromagnesian minerals.

Fig. 2. Simplified geological map of the eastern South Mountain Batholith (after MacDonald et al., 1988a) showing the location of the Halifax Pluton (HP), fine-grained leucomonzogranite and associated leucogranites (AL), and non-associated leucogranites (NL). Sample locations are for chemically analyzed samples discussed in text. The zonal arrangement of rock units in the HP (i.e. BMG–CGLMG–MBMG–CGLMG–BMG–BGD) is displayed in cross-section *A–B*.

TABLE 2

A summary of systematic petrographic variations for the sequence BGD-BMG-MBMG-CGLMG-PIN-FGLMG-AL-NL in the eastern SMB

Data Sets	Halifax Pluton				Leucogranite		
Rock Type	BGD	BMG	MBMG	CGLMG	PIN	FGLMG+AL	NL
Biotite	>25%						0%
Muscovite	tr						>25%
	repl			repl>euh		euh>repl	
Plagioclase	An>35						An<5
	zoned			zoned+unzoned		unzoned	
K-spar exsol	string			string+patch		nonexsolved	
Cordierite	tr	tr	tr-4%	tr-4%	tr-1%	tr	tr
Garnet	tr	tr	tr	tr	tr-4%	tr	tr
Andalusite	0	0	0	0-tr	0-tr	0-tr	0-2%
Topaz	0	0	0	0	0	0	0->1%

Abbreviations: BGD = biotite granodiorite; BMG = biotite monzogranite; MBMG = muscovite-biotite monzogranite; CGLMG = coarse-grained leucomonzogranite; PIN = polyphase intrusive suite; FGLMG = fine-grained leucomonzogranite; AL = associated leucogranite; NL = non-associated leucogranite; exsol, string, patch = albite exsolution textures; tr = trace; repl = anhedral muscovite replacing K-spar and other minerals; euh = euhedral muscovite (primary?); An = anorthite.

The distribution of these rock types is shown in Fig. 2. For a complete description of these rock types the reader is referred to MacDonald et al. (1988a, 1989).

A contoured density plot of 452 modal analyses from the SMB (Fig. 3a) indicates that the bulk of the SMB is monzogranite with lesser amounts of granodiorite and subordinate syenogranite and tonalite (fields after Streckeisen, 1976). A plot of the average QAP composition of each rock type (Fig. 3b) indicates a progressive increase in A/P (i.e. differentiation) from biotite granodiorite to leucogranite. Several petrographic features vary systematically in this sequence, and they are summarized in Table 2.

4. Sample selection and description of data sets

Ham et al. (1989) have analyzed 456 samples from the eastern SMB and present average major- and trace-element compositions for each of the seven main rock types shown in Fig. 2. Our subsets show the same increasing SiO_2, and incompatible trace elements (e.g. Rb, Ta, Nb, Li, F, Sn), and decreasing compatible trace elements (e.g. Ba, Sr, Zr, Sc, V, La) from biotite granodiorite to leucogranite as in the SMB as a whole.

The data sets used in this paper satisfy the following criteria: populations are large enough to be statistically valid; field relationships are well constrained; full petrographic information is available so that the statistical results could be discussed in terms of physical and chemical processes; and the range of compositions is representative of the entire SMB. We have selected three subsets (described below) that represent distinctly different geographic and/or lithological groupings in the SMB.

4.1. Halifax Pluton (HP)

The HP is a complexly zoned, cordierite-bearing plutonic complex that is exposed at the

TABLE 3

Average major- and trace-element compositions for the BGD, BMG, MBMG, and CGLMG from the HP, AL and NL from the eastern SMB. Sample locations are given in Fig. 1

Data set:	Halifax pluton:								Leucogranite:			
Rock type:	BGD		BMG		MBMG		CGLMG		AL		NL	
Number of samples:	10		19		23		25		18		34	
Source of data:	1		1		1		1		2,3		2,3	
	$\bar{X}$	SD	$\bar{X}$	SD	$\bar{X}$	SD	$\bar{X}$	SD	$\bar{X}$	SD	$\bar{X}$	SD
Major elements (%):												
SiO_2	68.11	0.71	69.55	0.80	71.33	1.34	72.95	0.80	74.67	0.76	73.78	0.97
TiO_2	0.59	0.02	0.44	0.07	0.40	0.08	0.20	0.07	0.11	0.05	0.06	0.03
Al_2O_3	15.52	0.37	15.10	0.31	14.49	0.41	14.32	0.33	14.04	0.45	14.64	0.53
$Fe_2O_{3(tot)}$	4.18	0.19	3.32	0.47	2.94	0.47	2.09	0.38	1.41	0.36	1.10	0.31
MnO	0.09	0.01	0.07	0.01	0.06	0.01	0.05	0.01	0.05	0.02	0.03	0.01
MgO	1.50	0.08	1.24	0.14	1.04	0.09	0.77	0.11	0.72	0.18	0.59	0.26
CaO	1.79	0.11	1.35	0.22	1.07	0.24	0.64	0.19	0.34	0.08	0.45	0.20
Na_2O	3.49	0.05	3.28	0.16	3.22	0.13	3.22	0.15	3.46	0.42	3.79	0.42
K_2O	3.80	0.13	4.49	0.32	4.40	0.16	4.66	0.18	4.40	0.20	4.11	0.36
P_2O_5	0.19	0.01	0.17	0.01	0.25	0.02	0.22	0.03	0.26	0.07	0.45	0.15
L.O.I.	0.65	0.12	0.64	0.13	0.71	0.10	0.63	0.11	0.70	0.17	0.87	0.27
Total	99.93	0.25	99.72	0.30	99.94	0.26	99.80	0.34	100.16	0.58	99.88	0.71
Trace elements (ppm):												
Ba	588	84	458	136	355	103	208	92	68	67	57	46
Rb	164	17	198	23	238	27	275	42	393	108	725	229
Sr	171	22	119	40	94	27	57	27	16	15	12	9
Hf	6	<1	4	1	4	1	3	1	1	1	1	1
Zr	177	14	138	22	132	19	86	23	53	16	31	16
Ta	1.1	0.2	1.2	0.5	1.7	0.3	1.8	0.5	3.0	1.2	7.0	4.2
Nb	12	1	11	1	14	1	11	1	13	4	23	8
Sc	9.4	1.2	6.6	1.5	5.9	1.1	4.0	0.8	3.2	1.0	2.6	1.3
V	44	5	28	7	28	8	12	6	4	4	2	2
La	34	3	26	7	24	4	15	5	7	4	4.5	8.3
Y	32	3	30	3	25	3	23	4	20	6	23	12
Th	12.3	1.3	11.3	1.2	11.3	1.4	8.3	2.0	4.8	1.6	5.0	8.1
U	3.0	0.5	3.3	0.8	4.3	1.5	5.8	2.5	7.4	5.3	4.4	3.0
Li	76	13	86	16	90	11	95	25	149	110	281	178
F	645	111	620	194	691	98	753	194	1199	888	2712	1082
B	26	8	25	11	30	6	34	23	29	9	19	8
As	4.6	7.2	2.0	3.3	2.2	1.1	3.7	3.6	6.1	8.6	2.0	1.2
Au (*ppb)	6	5	8	11	10	11	12	10	4	5	1	1
Sn	5	3	7	7	10	3	12	5	23	11	30	9
W	1	<1	1	3	2	1	2	2	8	9	8	3
Cu	1	3	3	3	1	3	0	1	1	3	2	3
Pb	23	6	25	6	26	15	21	3	19	5	13	7
Zn	70	12	65	21	71	43	51	15	46	24	56	21

Abbreviations: BGD = biotite granodiorite; BMG = biotite monzogranite; MBMG = muscovite–biotite monzogranite; CGLMG = coarse-grained leucomonzogranite; AL = associated leucogranite; NL = non-associated leucogranite; $\bar{X}$ = mean; SD = standard deviation.

Source of data: 1 = MacDonald and Horne (1988); 2 = Ham et al. (1989); 3 = D.B. Clarke (unpublished data).

eastern end of the SMB (Fig. 2). Average major- and trace-element contents for the BGD, BMG, MBMG and CGLMG from the HP (Table 3) are very similar to the average compositions of similar units in the eastern SMB (Ham et al., 1989). The HP comprises a normally zoned outer rim of BGD–BMG–CGLMG and a reversely zoned core of CGLMG–MBMG (MacDonald and Horne, 1988) as shown in the cross-section A–B in Fig. 2. The variation of Rb and Zr underscores the continuous chemical zonation of the HP (Fig. 4). From this pluton we have used all 77 available samples to represent the full range of its compositional variation.

4.2. Leucogranites from the eastern SMB

Leucogranites are the most chemically evolved rocks in the SMB, and they also display the greatest degree of deuteric alteration (e.g. albitization, muscovitization). Kontak et al. (1988) describe two types of leucogranite (Types I and II) based upon geochemistry and mineralogy. MacDonald et al. (1988a, b) have also described two types of leucogranite based upon field relationships, mineralogy and geochemistry. For the purpose of this paper, we use samples from two subsets of leucogranite corresponding to the two groups of MacDonald et al. (1988b). In all cases, samples were collected remote from any intense hydrothermal alteration.

*4.2.1. Associated leucogranites (*AL*)*

The first group of leucogranites occurs as small zones (generally < 100 m^2) and, therefore, they are too small to show on Fig. 2. These leucogranites are exclusively associated with fine-grained leucomonzogranites (FGLMG),

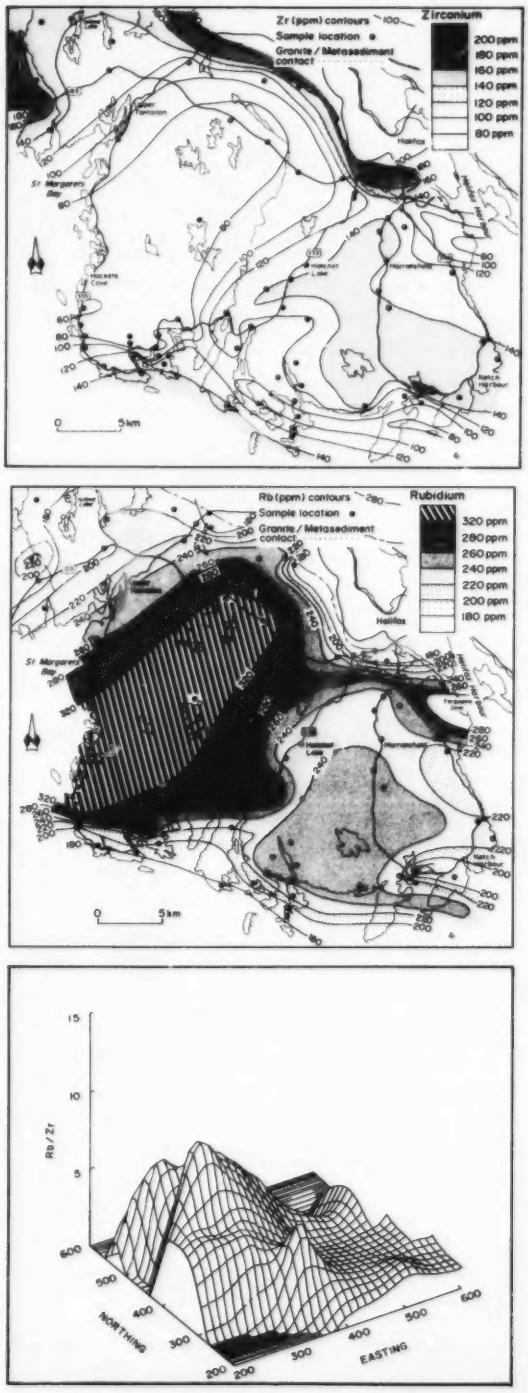

Fig. 4. Contour plots of Zr, Rb, and a 3-dimensional perspective plot of Rb/Zr for the HP (data from MacDonald and Horne, 1988). The isopleths show the regular variation in the Halifax Pluton, and the ratio Rb/Zr is simply a measure of overall differentiation, without being specific as to the processes involved.

show gradational contacts with FGLMG, and often display similar textures to their host rocks. This group of leucogranites is consequently termed associated leucogranites (AL). Although AL commonly resemble NL (below) in outcrop and hand sample, AL rocks are less evolved, with lower average levels of incompatible elements (in ppm, e.g. Rb 393, Ta 3, Nb 13, Li 149, F 1199, Sn 23) and higher contents of TiO_2 (0.11), Fe_2O_3 (1.41), MnO (0.05), MgO (0.72) and compatible trace elements (e.g. Ba 68, Sr 16, Zr 53, Sc 3.2, V 4, La 7) (Table 3). In addition, AL rarely contain andalusite or topaz and muscovite occurs mostly as anhedral replacement of K-feldspar with subordinate euhedral (primary?) grains. The AL are similar to the Type I leucogranites reported by Kontak et al. (1988). Eighteen representative samples from six AL bodies (Fig. 2) comprise this data set.

4.2.2. Non-associated leucogranites (NL)

Outcrop areas of the second group of leucogranites range in size from <1 to 5 km^2, and the bodies are invariably in sharp intrusive contact with a variety of host rocks (BGD, BMG, MBMG, CGLMG, FGLMG). Because of the absence of an association with any particular host rock, this group is termed non-associated leucogranites (NL). All NL bodies in the eastern SMB are shown in Fig. 2. Average major- and trace-element contents for NL (Table 3) indicate that this leucogranite group is the most evolved rock type in the eastern SMB, with the highest content of incompatible elements (e.g. Rb 725, Ta 7, Nb 23, Li 281, F 2712, Sn 30) and lowest content of TiO_2 (0.06), Fe_2O_3 (1.10), MnO (0.03) and MgO (0.59) and most compatible elements (Ba 57, Sr 12, Zr 31, Sc 2.6, V 2, La 4). Accessory minerals include andalusite, topaz and fluorite and euhedral (primary?) muscovite is more abundant than anhedral (replacement) muscovite. The NL are similar to the Type II leucogranite of Kontak et al. (1988). Thirty-four representative samples from the eleven NL bodies in Fig. 2 comprise the NL data set.

5. Spearman rank correlation coefficients (SRCCS)

We have calculated SRCCs for each of the three data sets (HP, AL and NL). The relative strength of each SRCC from the three matrices were then compared. Significant correlations ($|r_s| > 0.60$) were subsequently grouped into three categories: (1) strong correlation in HP, weak and not significant in NL ($\pm$AL); (2) strong correlation in NL ($\pm$AL), weak and not significant in HP; (3) moderate to strong and significant in HP, AL and NL. Each of these groups is briefly discussed below.

5.1. SRCCs *in the* HP

Figure 5a shows all SRCCs that are either moderate ($|r_s| = 0.60$–0.80) or strong ($|r_s| > 0.80$) in the HP data and not significant in the NL ($\pm$AL). Bivariate plots for four representative SRCCs (Ba–Sr, Ba–Zr, V–Sc and Sc–Sr) are shown in Fig. 6. The strength of the SRCC for each elemental pair has also been plotted as a bar graph (Fig. 6).

The SRCCs that distinguish the HP data set from the leucogranites (NL and AL) primarily involve positive correlations between elements that reside in the major mineral phases plagioclase (CaO, Sr), alkali feldspar (Ba), biotite (Sc, V, Fe_2O_3, TiO_2, MgO), and the accessory minerals zircon (Zr, Th, Hf), monazite (La, Th), and xenotime (Y). In addition, there are many negative SRCCs between the above suite of compatible elements and several incompatible elements including Rb, Ta, U, W and Sn. Strong negative SRCCs between SiO_2 and the compatible elements are also evident. In addition, there is no significant correlation involving Na_2O and P_2O_5, and K_2O shows weak negative SRCCs with Fe_2O_3, MnO, CaO, V, Hf and Sc, and a weak positive SRCC with Rb.

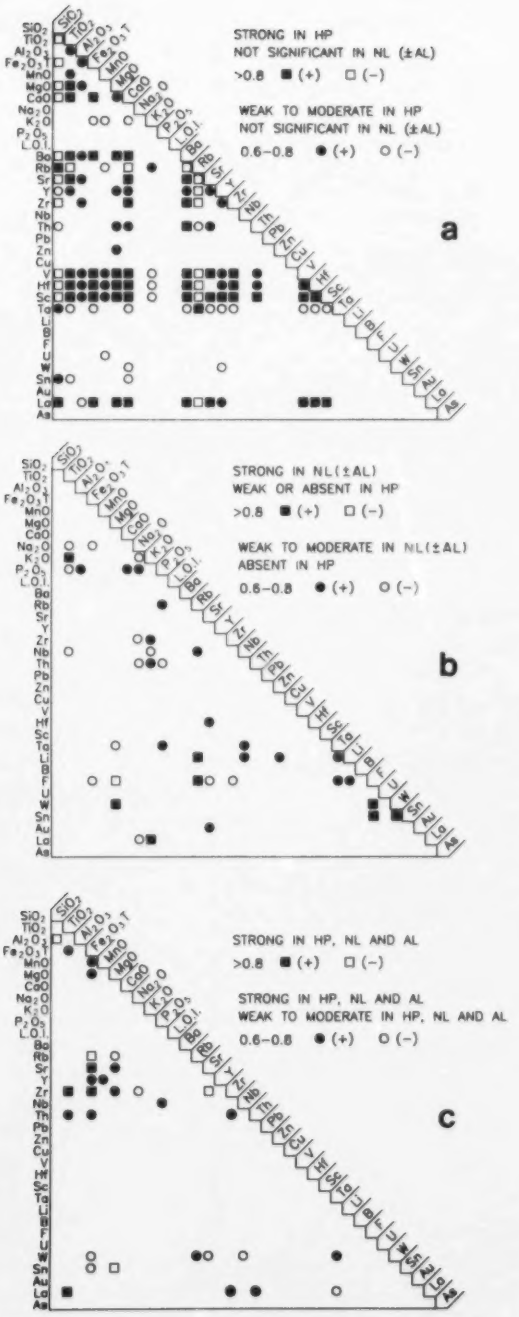
STRONG IN HP
NOT SIGNIFICANT IN NL (±AL)
>0.8 ■ (+) □ (-)
WEAK TO MODERATE IN HP
NOT SIGNIFICANT IN NL (±AL)
0.6–0.8 ● (+) ○ (-)
a
STRONG IN NL(±AL)
WEAK OR ABSENT IN HP
>0.8 ■ (+) □ (-)
WEAK TO MODERATE IN NL(±AL)
ABSENT IN HP
0.6–0.8 ● (+) ○ (-)
b
STRONG IN HP, NL AND AL
>0.8 ■ (+) □ (-)
STRONG IN HP, NL AND AL
WEAK TO MODERATE IN HP, NL AND AL
0.6–0.8 ● (+) ○ (-)
c

Fig. 5. Plot showing all SRCCs that are moderate ($|r_s| = 0.60$–0.80) or strong ($|r_s| > 0.80$) in: (a) the HP data, but not significant in the NL (±AL); (b) the NL (±AL), but not significant in the HP; and (c) the HP, AL, and NL data sets.

The strength of the above SRCCs in the AL data set are typically intermediate between the HP and NL sets. In fact several SRCCs that are very strong in the HP data (Fig. 5a) are also significant in the AL data set (e.g. Ba–Zr and V–Sc; Fig. 6).

5.2. SRCCs *in the leucogranites*

Figure 5b shows all SRCCs that are moderate ($|r_s| = 0.60$–0.80) or strong ($|r_s| > 0.80$) in the NL (±AL) data, but not significant in the HP data. Bivariate plots for four representative SRCCs (Rb–F, Sn–F, Na_2O–K_2O, P_2O_5–Al_2O_3) are shown in Fig. 7.

Simple inspection of Fig. 5, a and b, shows that the SRCCs that distinguish the NL (+AL) data sets from the HP data involve a much different suite of elements. Many of the correlations in the leucogranites involve incompatible elements that are strongly partitioned into the residual granite melt during crystallization, and are ultimately accommodated in muscovite (Rb, F, Li, Sn) or in their own mineral phases, for example cassiterite (Sn), fluorite, topaz or fluorapatite (F), wolframite (W) columbite–tantalite (Ta, Nb). Several compatible elements have moderate SRCCs; however, they are generally correlated with elements that were absent from Fig. 5a (e.g. P_2O_5, Na_2O, F, Li and Nb). Ta and Nb should behave coherently in all granitic rocks (Taylor, 1966); however, their positive SRCC is restricted to the NL and AL data (Fig. 5b). Na_2O and K_2O are poorly correlated with other elements in the HP, but they are moderately correlated with several elements in the NL (±AL) data set (e.g. Na_2O–P_2O_5, Na_2O–Th, Na_2O–La, K_2O–Zr, K_2O–Nb, K_2O–Th; Fig. 5b), and negatively correlated with each other in the leucogranites. P_2O_5 has low concentrations and is poorly correlated with other elements in the HP (Table 3; Fig. 5b), but is strongly enriched in the NL rocks with several significant SRCCs (e.g. P_2O_5–Al_2O_3, P_2O_5–Rb, P_2O_5–Th, P_2O_5–Ta; Fig. 5b).

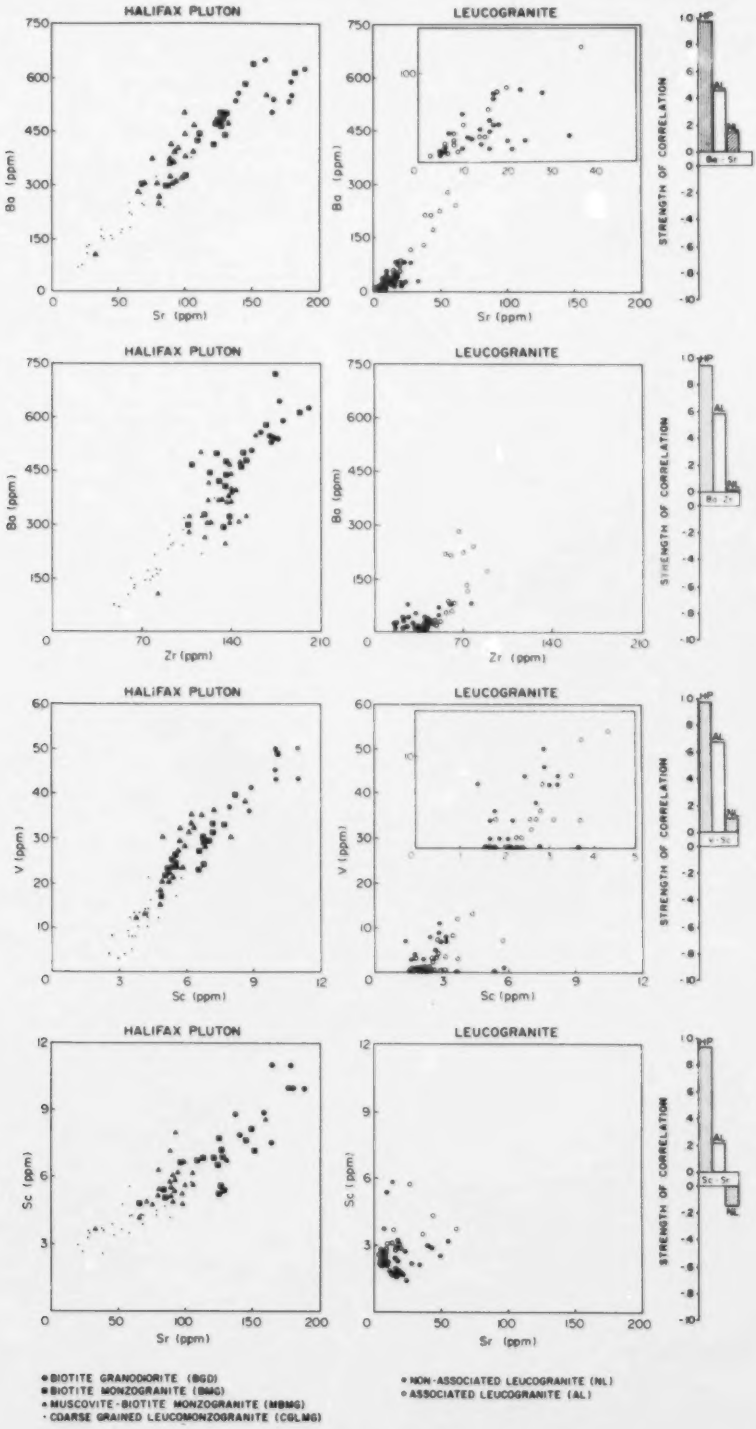

Fig. 6. Bivariate plots and associated SRCCs for Ba–Sr, Ba–Zr, V–Sc and Sc–Sr from the HP, AL, and NL data sets. See discussion in text.

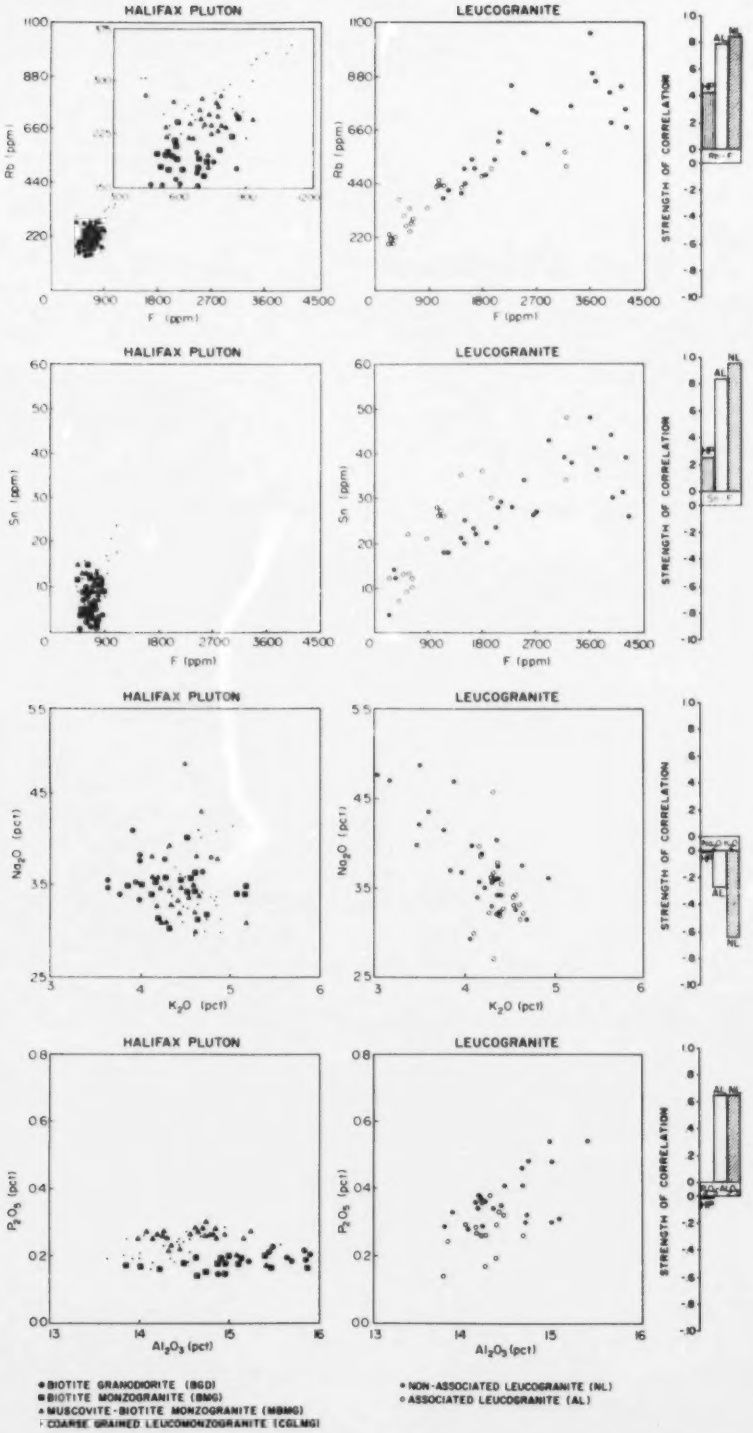

Fig. 7. Bivariate plots and associated SRCCs for Rb–F, Sn–F, Na_2O–K_2O and P_2O_5–Al_2O_3 from the HP, AL, and NL data sets. See discussion in text.

5.3. SRCCs *in* HP *and the leucogranites*

Several moderate to strong SRCCs are present in all three data sets (HP, AL, and NL) (Fig. 5c). Most of the SRCCs in Fig. 5c involve positive correlations between compatible elements (e.g. TiO_2–Fe_2O_3, –Zr, –Th, –La, Fe_2O_3–Sr, –Y, –Zr, MgO–Sr, –Zr, Th–Zr, La–Th) and, therefore, resemble the SRCCs in Fig. 5a. There are also several negative correlations between compatible and incompatible elements (e.g. Fe_2O_3–Rb, –W, –Sn, MgO–Rb, –Sn, Th–W, La–Ta; Fig. 5c) that resemble some of the SRCCs in Fig. 5a. There are only a few positive correlations between incompatible elements (e.g. W–Rb, Ta–W, P_2O_5–Nb; Fig. 5c) that resemble the SRCCs in the leucogranites (Fig. 5b).

6. Interpretation of the data

In this section we first consider a number of possible non-geological controls on the observed inter-element correlations, and then proceed to use the SRCCs to make geological inferences.

6.1. Non-geological controls on inter-element correlations

6.1.1. Closure

The problem of closure occurs when the sum of all the components measured in the analysis of an object is constant. An increase in one component necessitates a concomitant decrease in at least one other component and, therefore, no component varies independently (so-called "compositional data"). Whole-rock lithogeochemical analyses, by their nature, are susceptible to closure effects (Chayes, 1960). Aitchinson (1981, 1982) suggested that log-ratio or log-centering type transformations be applied to geochemical data sets to compensate for closure problems and non-normality in population distribution. Because we use non-parametric statistics, the use of logarithmic transformations is unnecessary and, as a consequence, we have transformed the data using $X_t = X_o/SiO_2$, where X_t is the transformed value of variable X, X_o is the original value of variable X that is divided by its corresponding value of SiO_2. The HP data set displays a much wider range of most major- and trace-element concentrations than the AL and NL data sets. If closure affected some SRCCs, these effects would be strongest in the HP data set, therefore only the HP data were considered in this section. All HP data were transformed using SiO_2, the major element with the widest variation (ca. 66–74%). Results from SRCC calculations for this transformed data set are graphically compared with SRCCs from uncorrected HP, AL, and NL data sets in Fig. 8. The transformed SRCCs for the HP data (e.g. Sc–Sr, Sc–La, V–Sc, Ba–Zr, Ba–Sr, V–Zr) clearly show no significant decrease from the original data. In fact, some SRCCs are strengthened, although these changes are probably statistically insignificant. Similarly, most of the major element SRCCs remain unchanged by the "closure" transformation. Notable exceptions are Al_2O_3–Fe_2O_3 which increases from $r_s = +0.60$ to $+0.80$, and K_2O–Fe_2O_3 which decreases from $r_s = -0.65$ to -0.35, indicating that closure may be a problem for some major element correlations. Trace element concentrations are presumably less affected by closure effects because of their low concentration. Their distribution will be more drastically affected by other physicochemical factors in the magma including elemental K_D's, magma concentration, types of complexing agents in magma (Cl, F, B, H_2O), polymerization/depolymerization within the melt, H_2O content, P–T, etc.

6.1.2. Comparing rock types with varying compositional ranges

Most SRCCs that distinguish the HP from NL and AL involve compatible elements. In the HP, modal amounts of biotite (with inclusions

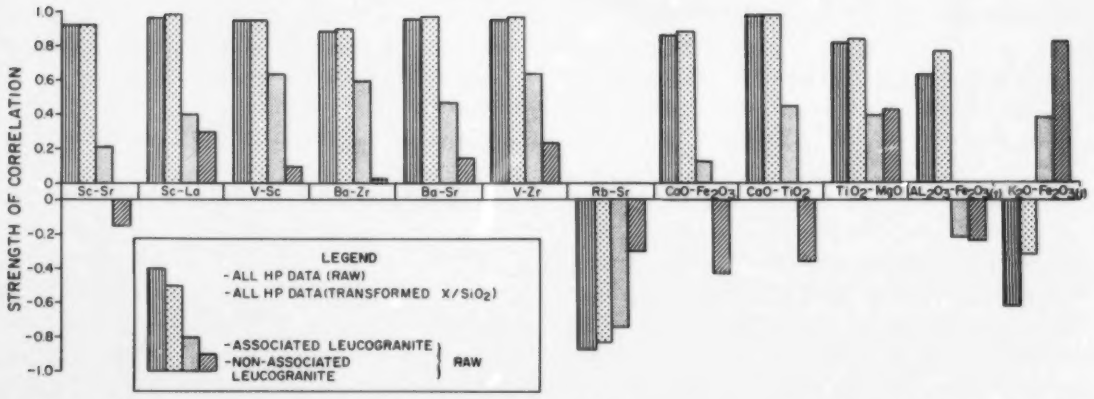

Fig. 8. SRCCs for raw data from the HP compared with SRCCs for data after a correction for closure (x/SiO_2). SRCCs for the AL and NL data have been included for comparison. With the exception of an increase in Al_2O_3–Fe_2O_3 and a decrease in K_2O–Fe_2O_3, most major- and trace-element SRCCs are unaffected by the data transformation, indicating that closure effects do not contribute to the strength of SRCCs in the HP.

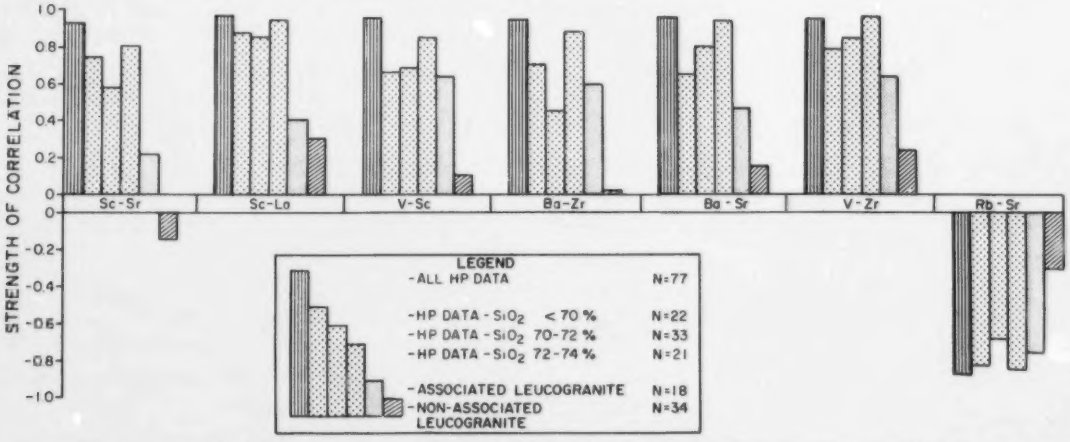

Fig. 9. SRCCs for raw HP data compared with subsets of the HP data (SiO_2 < 70%, 70–72%, and 72–74%) to evaluate the effect of restricted compositional range on inter-element correlation. SRCCs for the AL and NL data are plotted for comparison. There is a slight reduction in SRCC strength in the SiO_2 < 70% and 70–72% groups, whereas the 72–74% subset has SRCCs that approach the entire HP data set.

of zircon, monazite, apatite and rutile) vary from approximately 20% in BGD to <4% in CGLMG. This sharply contrasts with the 0–2% range for modal biotite in the majority of the leucogranites. The paucity of significant SRCCs for the compatible elements (e.g. Ba, Sr, Th, La, Zr, Y) in the NL (±AL) data might simply reflect the low concentration and restricted modal range of the host mineral phases.

To evaluate if these discrepancies in compositional ranges between rock types produced distinctions that were more apparent than real, we have divided the HP into compositionally restricted subgroups. We created three subsets corresponding to SiO_2 < 70%, 70–72% and 72–74%. Intervals of 2% SiO_2 were selected to approximate the SiO_2 range in the leucogranite data as indicated by the standard deviations for

NL and AL in Table 3 (0.97 and 0.76, respectively)

We calculated SRCCs for the three HP subsets and compared the results with the original correlations from the HP, AL and NL data sets. Several strong SRCCs (Sc–Sr, Sc–La, V–Sc, Ba–Zr, V–Zr and Rb–Sr) for the above groups are presented in Fig. 9. There is minor degradation in the strength of all SRCCs in both the SiO_2 <70% and 70–72% subsets, whereas correlations in the 72–74% subset approach those of the complete HP data set. With the exception of Ba–Zr in the 70–72% SiO_2 subset (SRCC=0.46), all of the Fig. 9 correlations, for the HP subsets, are significant ($|r_s| > 0.60$) and greatly exceed the non-significant correlations in the NL data. Therefore, varying compositional ranges between the rock types do not substantially contribute to the variances in inter-elemental behaviour between these rock types.

6.1.3. Contiguous versus composite data sets

The SMB is a composite batholithic complex that comprises numerous coalesced plutonic bodies with unique petrological and geochemical characteristics (Smith, 1979; MacDonald et al., 1988a; Corey, 1988; Horne et al., 1989) and economic potential (Smith and Turek, 1976; Chatterjee et al., 1983). The HP data set is composed entirely of samples from one of these plutons, whereas the AL and NL samples were collected from several plutons. Therefore, we considered the possibility that the observed differences in SRCC signatures between HP, AL and NL may have been caused by comparing data drawn from a single pluton, as opposed to data drawn from several. To test this potential problem, a new composite data set containing 59 samples of granodiorite and monzogranite from all plutons of the eastern SMB was compiled from Ham et al. (1989).

We calculated SRCCs for the composite data set and compared the results with the HP, AL, and NL data and plotted representative correlations in Fig. 10. The strong SRCCs of Fig. 5a show minor deterioration in the composite granodiorite–monzogranite data set (e.g. Sc–Sr, Sc–La, Ba–Zr and Rb–Sr in Fig. 10). However, virtually all of the SRCCs in this composite data set exceed 0.60 and are significantly higher than the NL ($\pm$AL) data sets (Fig. 10). The reduction in the strength of the SRCCs presumably reflects slight geochemical variations between individual plutons (Smith, 1979; Horne et al., 1989). The strong SRCCs in the NL data (Fig. 5b) are very weak and not significant (<0.20) in the composite granodiorite–monzogranite group (e.g. F–W, F–Sn and Zn–Li; Fig. 10). Thus the different SRCC signatures of the HP, AL and NL do not result from a comparison of homogeneous (HP) and composite data sets (AL and NL). This discussion does not, however, preclude the possibility that significant correlations could exist between elements in individual bodies of AL or NL, but the numbers of samples from individual bodies are currently too small to show them.

6.1.4. Detection limits and analytical variance

Analytical variance for both major and trace elements increases at low concentrations, especially at levels approaching the detection limits for the specific analytical techniques (Levinson, 1974; Rose et al., 1979). Increased analytical variance at very low concentrations will produce increased scatter and poorer inter-elemental correlations. There are significant compositional differences between the HP and leucogranitic rocks (Table 3) as discussed above. For example, the HP is relatively depleted in the incompatible elements (e.g. Ta 1.1–1.8 ppm, W 1–2 ppm), whereas the NL is relatively depleted in the compatible elements (e.g. Hf 1 ppm, V 2–4 ppm). Some of the observed differences in SRCC signatures between the data sets may be caused by these low concentrations, but most elements are sufficiently enriched above the lower limits of de-

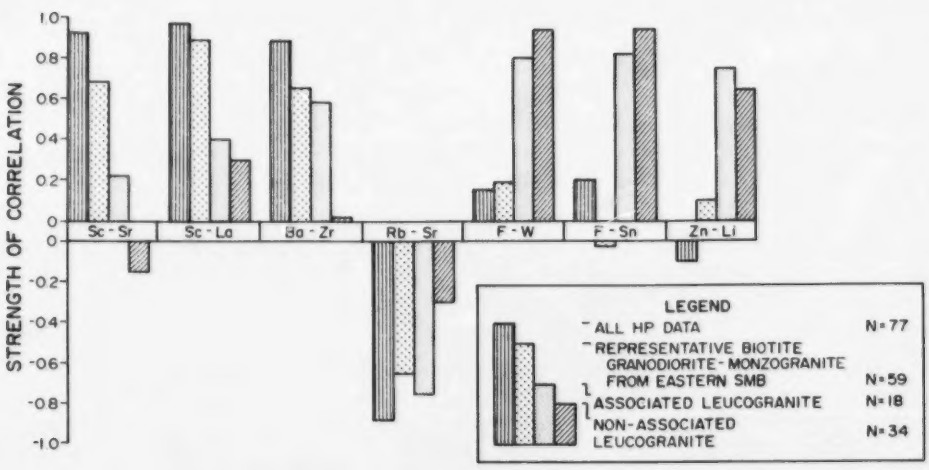

Fig. 10. SRCCs for the HP, AL, and NL data sets compared with a composite group of granodiorites and monzogranites from several plutons in the entire eastern SMB (data from Ham et al., 1989).

tection that analytical variance should not be a problem.

6.1.5. Conclusions concerning non-geological controls

We have evaluated the possible effects of closure (constant sum), variable compositional ranges, contiguous vs. composite data sets, and differing analytical precisions on the values of the SRCCs and conclude that none of these factors significantly affects the inter-element correlations in the three subsets of samples. The observed correlations, therefore, must have geological control and significance.

6.2. Geological controls on inter-element correlations

In this section, we use field, petrographic, and other geochemical observations in an attempt to attach geological meaning to the inter-element correlations.

6.2.1. Halifax Pluton

Using conventional chemical variation diagrams, McKenzie and Clarke (1975), Smith et al. (1986), and MacDonald and Horne (1988) concluded that removal of plagioclase, alkali feldspar, biotite and accessory zircon, monazite, xenotime, apatite and rutile by fractional crystallization explained the compositional variations in the HP. This process must produce strong positive correlations for elements that co-exist in one or more of the above minerals such as Sc and V in biotite or CaO and Sr in plagioclase. Strong positive SRCCs for elements that reside in different mineral phases (e.g. Ba–Zr, Sc–Sr; Fig. 6) indicate that the removal of these minerals by fractional crystallization must have been monotonic (i.e. no reversals in the depletion trends). Incompatible elements (e.g. Rb, Ta), by definition, must accumulate in the residual melt that is produced during fractional crystallization and should, therefore, produce negative SRCCs with the compatible elements (e.g. V, Hf, Sc). Therefore, virtually all of the moderate and strong SRCCs that distinguish the HP from the highly evolved leucogranites (Fig. 5a) can be explained by the process of fractional crystallization as suggested by Smith et al. (1986) and MacDonald and Horne (1988).

Alteration features (e.g. albitization, K-feldspathization, muscovitization) increase in in-

tensity from the biotite granodiorite to the coarse-grained leucomonzogranite in the HP (MacDonald and Horne, 1988); however, the strong SRCCs in Fig. 5a commonly approach +1 or −1 (Fig. 6). This suggests that either the bulk chemical alteration effects were slight (elements were simply relocated in the same volume of rock), or that the strongly correlated element pairs are contained in resistant phases (e.g. monazite and zircon), or both.

6.2.2. Leucogranites

On the basis of petrographic observations and chemical variation diagrams, Muecke and Clarke (1981), Clarke and Chatterjee (1988), and Kontak et al. (1988) concluded that late-magmatic and/or post-magmatic processes involving fluids were major contributors to the variation in chemical compositions of the evolved leucogranites and mineral deposits. However, the complete cohort of elements involved in these processes was not defined. By isolating the two leucogranite types, and comparing them with the HP data, we can begin to define the transition between variation attributable to fluid-absent magmatic processes, and those attributable to fluid-present hypersolidus and subsolidus processes.

The strong SRCCs in the NL suite (Fig. 5b), combined with the petrographically observed albitization and K-feldspathization, also immediately suggest control by hydrothermal alteration. Thus, volatile-rich fluids transporting the suite of elements in Fig. 5b may have prevented and/or obliterated some of the magmatic signatures, and created strong new correlations of their own.

Individual SRCCs in the AL data are commonly intermediate between the HP and NL data sets (Fig. 5b). This is consistent with the observation above that AL rocks resemble their spatially related fine-grained leucomonzogranite hosts, despite their degree of alteration. The significant positive correlations between compatible elements (e.g. Ba–Zr, V–Sc; Fig. 6) that are attributed to fractional crystallization in the HP indicates that the hydrothermal alteration was unable to decouple these element pairs. Significant reductions in other strong SRCCs (e.g. Sc–Sr) presumably reflects a reduction in the magmatic correlations by invading fluids. The moderate to strong positive SRCCs for several incompatible elements (e.g. Rb–F, Sn–F, P_2O_5–Al_2O_3) in the AL rocks suggests a significant contribution from fluids (e.g. the mobility of Al in altered SMB rocks has been shown by Corey, 1988). The AL rocks represent the pivotal point in the evolution of the SMB where magmatic correlations yield to late-magmatic or post-magmatic ones involving fluids.

6.2.3. Halifax Pluton and leucogranites

Moderate to strong SRCCs in all three data sets (Fig. 5c) primarily involve compatible/compatible (positive correlations) and compatible/incompatible (negative correlations) element pairs as in the HP (Fig. 5a). The positive SRCCs in the post-magmatically altered NL suggest either that the corresponding mineral phases (e.g. zircon–Zr, Th; monazite–La, Th; xenotime–Y) were impervious to the invading hydrothermal fluid, or that their breakdown and release of elements by alteration was accompanied by their accommodation in secondary mineral phases (e.g. muscovite).

The negative SRCCs in Fig. 5c suggest that the compatible/incompatible behaviour of given element pairs (e.g. MgO–Sn, Fe_2O_3–Rb) is maintained in the NL rocks, only here the removal of compatibles and concentration of incompatibles was controlled by a fluid rather than fractional crystallization. None of the SRCCs in Fig. 5c can be uniquely ascribed to either magmatic or post-magmatic processes and are not, therefore, useful for determining the mechanism of chemical control.

7. Summary and conclusions

Nonparametric statistical techniques are particularly useful for geological data sets that

commonly display non-Gaussian distributions. We have established that SRCCs can characterize the geochemical signature of well constrained rock subsets from the SMB and, from combinations with other observations, we can consequently use the SRCCs to evaluate the relative contribution of magmatic versus post-magmatic processes to the chemistry of these rocks.

Samples from the magmatic suite in the HP have several inter-element SRCCs that approach $|r_s| = 1$ as expected for fractional crystallization. The observed deuteric alteration that increases from BGD to CGLMG in the HP did not significantly change the magmatic SRCCs, suggesting that the mineral phases containing these elements were not significantly affected by the alteration.

The two leucogranitic suites have very different SRCC signatures. The associated leucogranites (AL) have several significant magmatic SRCCs despite moderate to extensive alteration (muscovitization, chloritization, albitization, K-feldspathization), and very low modal amounts of biotite and included accessories. The observed degradation in strength of SRCCs presumably reflects significant alteration but may also reflect the restricted compositional range and composite nature of this data set. The non-associated leucogranites (NL) show strong SRCCs involving incompatible elements that were enriched in a fluid phase and deposited through fluid/melt and/or fluid/rock interaction. Intensely altered zones, that are commonly associated with granophile mineralization, were avoided during sampling (Ham et al., 1989). Attainment of perfect correlation ($|r_s| = 1$) resulting from intense alteration would therefore be unlikely. The SRCCs in the NL data set rarely exceed $|r_s| = 0.80$ and reflect the incomplete hydrothermal alteration of the NL rocks.

Granophile mineralization is both spatially and genetically related to highly evolved "specialized" granites (Tischendorf, 1977) or "para-intrusive" rocks (Clarke and Chatterjee, 1988) that, by definition, are granitoid rocks with compositional variation trends drastically different from co-magmatic rocks. Clearly, NL satisfies the criteria for "specialized granite" more than AL. Several mineral deposits in the SMB are associated with NL rocks; therefore, proper classification of any newly discovered leucogranites in the SMB will have a bearing on their assessment for mineralization. Our work indicates that a SRCC matrix for a suite of major and trace elements similar to that used in this study, for a small sample set (e.g. $N = 18$) will correctly classify any leucogranite as AL or NL.

In the general case, each geological process must be characterized by a unique matrix of Spearman rank correlation coefficients equal to +1 (compatible–compatible, or incompatible–incompatible element pairs), or −1 (compatible–incompatible element pairs). Simple chemical modelling could be used to define the SRCC matrix for each process (e.g. fractional crystallization of biotite + plagioclase + zircon, or greisenization) and, once the matrices were so defined, they could be used directly to identify processes in unknown suites. Even combinations of processes could be identified (e.g. fractional crystallization overprinted by greisenization, in which the SRCCs will remain equal to unity for some element pairs, but will become less than one for others).

In conclusion, Spearman rank correlation coefficients can be used with compositional data drawn from populations with non-normal distributions to provide a *comprehensive and rapid*, non-graphical assessment of inter-element correlations, to quantify these inter-element relationships, and to both identify processes, and to gauge their relative contributions to the observed compositions. Key correlation coefficients might also be used quantitatively to assess the economic potential of leucogranite suites in the SMB and elsewhere.

Acknowledgements

We wish to acknowledge the interest and support of Angelo Peccerillo for our work, and the helpful comments offered by two reviewers, F.A. Frey and D. Garcia. We acknowledge also the substantial contribution of R.J. Horne, M.C. Corey, and L.J. Ham in the regional mapping program in the South Mountain Batholith from 1984 to 1989, and the financial support of it by the Canada–Nova Scotia Mineral Development Agreement. D.B. Clarke also acknowledges a grant in aid of research from the Natural Sciences and Engineering Research Council of Canada. The authors also thank J. Campbell and staff in the drafting section of NSDME for preparation of the figures.

References

Aitchinson, J., 1981. A new approach to null correlations of proportions. J. Math. Geol., 13: 175–189.

Aitchinson, J., 1982. The statistical analysis of compositional data. R. Stat. Soc. J., B, 44: 139–177.

Chatterjee, A.K., Strong, D.F. and Muecke, G.K., 1983. A multivariate approach to geochemical distinction between tin-specialized and uranium-specialized granites of southern Nova Scotia. Can. J. Earth Sci., 20: 420–430.

Chayes, F., 1960. On correlation between variables of constant sum. J. Geophys. Res., 65: 4185–4193.

Clarke, D.B. and Chatterjee, A.K., 1988. Physical and chemical processes in the South Mountain Batholith. In: R.P. Taylor and D.F. Strong (Editors), Recent Advances in the Geology of Granite-Related Mineral Deposits. Can. Inst. Min. Metall. Spec. Vol., 39: 223–233.

Clarke, D.B. and Muecke, G.K., 1985. Review of the petrochemistry and origin of the South Mountain Batholith and associated plutons, Nova Scotia, Canada. In: High Heat Production (HHP) Granites, Hydrothermal Circulation and Ore Genesis. Institution of Mining and Metallurgy, London, pp. 41–54.

Corey, M.C., 1988. An occurrence of metasomatic aluminosilicates related to high alumina hydrothermal alteration within the South Mountain Batholith, Nova Scotia. Marit. Sediments Atl. Geol., 24, 83–95.

Gibbons, J.D., 1971. Nonparametric Statistical Inference. McGraw-Hill, Kogakusha, Tokyo.

Graves, R.M., MacDonald, M.A., Finck, P.W. and Boner, F.J., 1988. A comparison of the clast composition and geochemistry of granite tills to underlying bedrock in the Halifax Pluton, central Nova Scotia. In: D.R. MacDonald and K.A. Mills (Editors), Prospecting in Areas of Glaciated Terrain. Can. Inst. Min. Metall., Halifax, N.S., pp. 21–39.

Ham, L.J., Marsh, S.W., Corey, M.C., Horne, R.J. and MacDonald, M.A., 1989. Lithogeochemistry of the eastern portion of the South Mountain Batholith, Nova Scotia. Nova Scotia Department of Mines and Energy Open File Report 89-001, 62 pp.

Henley, S., 1981. Nonparametric Statistics. Elsevier, Amsterdam, 145 pp.

Horne, R.J., Corey, M.C., Ham, L.J. and MacDonald, M.A., 1989. Lithogeochemical variation in biotite monzogranite and biotite granodiorite of the South Mountain Batholith, southwestern Nova Scotia. In: Program with Abstracts, Atlantic Geoscience Society Colloquium '89, Amherst, N.S.

Kontak, D.J., Strong, D.F. and Kerrich, R., 1988. Crystal-melt+fluid phase equilibria versus late-stage fluid–rock interaction in granitoid rocks of the South Mountain Batholith, Nova Scotia: whole-rock geochemistry and oxygen isotope evidence. Marit. Sediments Atl. Geol., 24: 97–110.

Levinson, A.A., 1974. Introduction to Exploration Geochemistry. Applied Publishing Ltd., Maywood, Ill., 614 pp.

MacDonald, M.A. and Horne, R.J., 1988. Petrology of the zoned, peraluminous Halifax Pluton, south-central Nova Scotia. Marit. Sediments Atl. Geol., 24: 33–46.

MacDonald, M.A., Corey, M.C., Ham, L.J. and Horne, R.J., 1988a. South Mountain Batholith project: a progress report on bedrock mapping. In: D.R. MacDonald and Y. Brown (Editors), Mines and Minerals Branch, Report of Activities 1988, Part A. Nova Scotia Department of Mines and Energy, Report 88-3, pp. 109–116.

MacDonald, M.A., Corey, M.C., Ham, L.J. and Horne, R.J., 1988b. Leucogranite and leucomonzogranite in the South Mountain Batholith, southwestern Nova Scotia. In: Programs with Abstracts, Atlantic Geoscience Society Colloquium '88, Antigonish, N.S.

MacDonald, M.A., Corey, M.C., Ham, L.J. and Horne, R.J., 1989. Petrologic and geochemical aspects of the South Mountain Batholith. In: D.R. MacDonald (Editor), Mines and Minerals Branch, Report of Activities 1989, Part A. Nova Scotia Department of Mines and Energy Report 89-1.

McKenzie, C.B. and Clarke, D.B., 1975. Petrology of the South Mountain batholith, western Nova Scotia. Can. J. Earth Sci., 12, 1209–1218.

Muecke, G.K. and Clarke, D.B., 1981. Geochemical evolution of the South Mountain Batholith, Nova Scotia: rare-earth element evidence. Can. Mineral., 19: 133–145.

O'Connor, P.J., Reimann, C. and Kuerzl, H., 1988. An application of exploration data analysis (EDA) techniques to stream sediment surveys for gold and asso-

ciated elements in the county Donegal, Ireland. In: D.R. MacDonald and K.A. Mills (Editors), Prospecting in Areas of Glaciated Terrain. Canadian Institute of Mining and Metallurgy, Montréal, Qué., pp. 449–468.

Richard, L.R. and Clarke, D.B., 1989. Multivariate statistical models for granites in terrane analysis: Nova Scotia, Morocco, and Iberia. Geol. Soc. Am. Bull., 101: 1157–1162.

Rogers, P.J. and MacDonald, M.A., 1984. Stream sedimennt sampling, orientation studies and geochemical associations from selected deposits on Cape Breton Island, Nova Scotia. In: Current Research, Part B. Geol. Surv. Can., Pap., 84-1B: 65–74.

Rogers, P.J., Stea, R.R. and MacDonald, M.A., 1984. Statistical investigation of the geochemical reflection of Au mineralization in the tills and lake sediments of the Eastern Shore Region of Nova Scotia. In: M.J. Jones (Editor), Prospecting in Areas of Glaciated Terrain. Institution of Mining and Metallurgy, London, pp. 137–152.

Rose, A.W., Hawkes, H.E. and Webb, J.S., 1979. Geochemistry in Mineral Exploration. Academic Press, London, 657 pp.

Siegel, S., 1956. Nonparametric Statistics for the Behavioral Sciences. McGraw-Hill, New York, N.Y.

Smith, T.E. 1979. The geochemistry and origin of the Devonian granitic rocks of southwest Nova Scotia. Geol. Soc. Am. Bull., Part 2, 90: 850–885.

Smith, T.E. and Turek, A., 1976. Tin-bearing potential of some Devonian granitic rocks in southwest Nova Scotia. Miner. Deposita, 11: 234–245.

Smith, T.E., Peck, D., Huang, C.H. and Holm, P.E., 1986. A re-appraisal of the alaskite/muscovite–biotite granite suite of Halifax County, Nova Scotia. Marit. Sediments Atl. Geol., 22: 101–116.

Streckeisen, A.L., 1976. To each plutonic rock its proper name. Earth-Sci. Rev., 12: 1–33.

Taylor, R.S., 1966. The application of trace element data to problems in petrology. Phys. Chem. Earth, 6: 133–213.

Tischendorf, G., 1977. Geochemical and petrographic characteristics of silicic magmatic rocks associated with rare element mineralization. In: M. Stemprok, L. Burnol and G. Tischendorf (Editors), Metallization Associated with Acid Magmatism. Geological Survey of Prague, Prague, 2: 41–96.

Wilkinson, L., 1988. SYSTAT: The System for Statistics. SYSTAT, Inc., Evanston, Ill.

Yule, G.U. and Kendall, M.G., 1965. An Introduction to the Theory of Statistics. Charles Griffin, London, 701 pp.